

Property and Microstructure of TiNi SMA Prepared Using BaZrO₃ Crucible

Gao Pengyue¹, Li Zheng¹, Zhu Ming³, Chen Guangyao¹, Wajid Ali¹, Li Mingyang¹, Qin Ziwei^{1,2}, Wang Hongbin^{1,2}, Lu Xionggang^{1,2}, Li Chonghe^{1,2}

¹ State Key Laboratory of Advanced Special Steel & Shanghai Key Laboratory of Advanced Ferrometallurgy, Shanghai University, Shanghai 200072, China; ² Shanghai Special Casting Engineering Technology Research Center, Shanghai 201605, China; ³ General Research Institute for Non-Ferrous Metals, Beijing 100088, China

Abstract: TiNi shape memory alloy (SMA) is one of the commercially successful shape memory alloys (SMAs) due to its excellent performances. The 49.3Ti-Ni (at%) alloy was prepared by vacuum induction melting in a 25 kg-grade home-made BaZrO₃ crucible, and the alloy ingot was turned into wire form (Φ 1.0 mm). The chemical compositions (including oxygen, nitrogen and carbon) of the as-cast alloy were measured and the phase constitution was analyzed by X-ray diffraction (XRD). The microstructures were observed by optical microscope (OM) and scanning electron microscope (SEM), and the shape memory recovery rate and fatigue life of alloy wires were tested by two home-made test apparatus, respectively. Experimental results show that the contents of oxygen and nitrogen in the alloy ingot are 560 and 17 μ g/g, respectively, and the impurity contents in TiNi alloy melted using the BaZrO₃ crucible are just eligible to medical devices and surgical implants. The TiNi alloy chemical composition has a more uniform and accurate melted using BaZrO₃ crucible than alloy prepared by the vacuum arc remelting (VAR), and has a higher shape memory recovery rate and fatigue life than the alloy melted using graphite crucible. The best shape memory recovery rate can reach 98.62% under 2% deformation after aging at 550 °C for 20 min and water quenching, and the best average fatigue life can reach 3072 times after aging at 500 °C for 20 min and water quenching.

Key words: BaZrO₃ crucible; TiNi shape memory alloy; microstructure; property

Numerous investigations have been conducted on shape memory alloys (SMAs) as a class of functional materials exhibiting unique characteristic properties under external stimuluses such as thermal, mechanical and magnetic fields^[1,2]. Among SMAs, TiNi alloy system has attracted many researchers because of its superior shape memory effect (SME) and superelasticity (SE), better mechanical properties, higher corrosion resistance and excellent biocompatibility^[3-6]. However, these properties strongly depend on the accurate chemical composition, processing techniques and impurity contents^[7]. Some investigations^[8-10] have indicated that contaminants, such as oxygen and carbon, can severely deteriorate the mechanical, fatigue and shape memory properties of TiNi alloys, and their penetration mainly occurs during the production and melting.

Different methods have been used to produce TiNi SMA for experimental purposes^[11,12]. However, only vacuum induction melting (VIM) and vacuum arc remelting (VAR) are widely used in commercial production. In VAR, the melting and solidification process takes place in the water-cooling copper crucible, effectively avoiding from the crucible contaminants. However, since the melting and solidification are confined in a small molten pool, the ingot melted by the VAR method lacks chemical homogeneity. Even the large melting pool and magnetic stirring have been employed in the commercial VAR melting process, and the solidification skull caused by the cooling water still cannot be thoroughly stirred. Generally, it is necessary to melt the ingot several times to ensure chemical homogeneity. Moreover, the cooling water consumes a large amount of

Received date: January 25, 2018

Foundation item: National Natural Science Foundation of China (51374142, U1760109)

Corresponding author: Li Chonghe, Ph. D., Professor, School of Materials Science and Engineering, Shanghai University, Shanghai 200072, P. R. China, Tel: 0086-21-56332934, E-mail: chli@staff.shu.edu.cn

Copyright © 2019, Northwest Institute for Nonferrous Metal Research. Published by Science Press. All rights reserved.

heat during the melting process, which results in a much higher cost compared to VIM.

In VIM, the electrodynamic forces constantly stir the molten metal, thus ensuring greater chemical and microstructural homogeneity in the ingot. The major shortcoming in VIM is the inherent reaction between the melt and the crucible because of the high chemical activity of titanium alloys. The graphite crucible has been widely used for vacuum induction melting so far. However, the carbon contaminant from the graphite crucible can deteriorate the mechanical and shape memory properties. Numerous investigations have been concentrated on less contaminating crucible materials, such as BN, AlN, Y_2O_3 and ZrO_2 ^[13-16], which are used to melt this alloy. Unfortunately, the satisfactory results are rarely presented^[17]. Moreover, the CaO crucible is used to melt titanium alloys due to its refining effects such as de-oxidation, de-sulfurization and de-nitritification^[18]. However, CaO is still not an ideal refractory material because of its poor hydration resistance.

$BaZrO_3$ is a typical cubic perovskite with a melting temperature of 2600 °C, and presents good mechanical strength, high thermal and chemical stability, and a low coefficient of thermal expansion^[17,19,20]. In our previous work^[17], this crucible was investigated for re-melting TiNi master alloy, and it was found that the $BaZrO_3$ crucible possesses poor wettability and inertness to the melting of TiNi alloy, and no reaction and diffusion layer can be found between the melt and the crucible. Meanwhile, according to our previous study^[21], the 25 kg-grade home-made $BaZrO_3$ crucible was successfully prepared. The purpose of this study is to melt the TiNi alloy using home-made $BaZrO_3$ crucible and analyze its chemical composition, shape memory effect and fatigue behavior, and compare with the counterpart of the graphite crucible. The results may provide a preliminary assessment of the properties and microstructures of TiNi alloys prepared using $BaZrO_3$ crucible.

1 Experiment

1.1 Preparation of the Crucible

The preparation method of $BaZrO_3$ crucible was reported in our previous work^[17]. In the following work, it was optimized to make the crucible more fit for the industrial production^[21]. The process for making the $BaZrO_3$ crucible can be divided into the following three stages, namely preparation of the fused $BaZrO_3$, shaping of the crucible and the sintering of the crucible.

In the first stage, the fused $BaZrO_3$ was produced in an electric arc furnace by adding $BaCO_3$ (the average particle size is 7.3 μm , industrial grade) and ZrO_2 (the average particle size is 3.6 μm , industrial grade) into a Higgins furnace. The $BaCO_3$ and the ZrO_2 powders were mixed precisely at 1.0:1.51 molar ratios. This process was maintained for 12 h

to produce the fused $BaZrO_3$ and a spot of ZrO_2 ^[22]. The X-ray diffraction (XRD) peaks in Fig.1 reveal the $BaZrO_3$ and ZrO_2 as present phases.

Subsequently, the fused $BaZrO_3$ particles with an average particle size is 0~3 mm (the percentage of fused particle with 0~1 mm particle size is 40% and others is 1~3 mm) were screened out. After that, the fused $BaZrO_3$ with an average particle sizes are 0~1 mm and 1~3 mm was mixed at 1:2 volume ratio. The home-made powder was shaped into a rubber mould, and the green body was formed at 180 MPa by cold isostatic pressing for 15 min. Finally, the green body was sintered at 1720 °C for 6 h.

1.2 Melting Process

49.3Ti-Ni (at%) SMA was prepared using the titanium sponge named 0 grade (99.7%) with a mass of 5.97 kg and the electrolysis nickel plate (99.96%) with a mass of 7.53 kg as raw materials. Before the melting process, the raw materials were dried in a muffle furnace at 150 °C for 24 h.

After the drying procedure, the titanium sponge was placed in the center of crucible and the nickel plates were placed around the titanium sponge, in order to avoid the direct interaction between the crucible and the titanium sponge. Thus, the assembling sequence of loading structure from outside to inside is coil, asbestos cloth, magnesia, crucible, electrolysis nickel and titanium sponge in turn, which is illustrated in Fig.2. Nayan et al.^[23] found that this arrangement avoid the direct contact between the graphite crucible and titanium effectively, resulting in a substantial reduction in carbon contents in the ingot. Similar experimental results were also obtained in the $BaZrO_3$ crucible. Since the nickel melts at a lower temperature than that of the titanium, the above charging sequence will ensure that the solid titanium is always encased by liquid nickel till it melts and goes into the solution^[23].

In this experiment, the melting process in the vacuum induction furnace was operated using the 25 kg-grade home-made $BaZrO_3$ crucible under the atmosphere of argon gas with a purity of 99.99%. The furnace was purged with

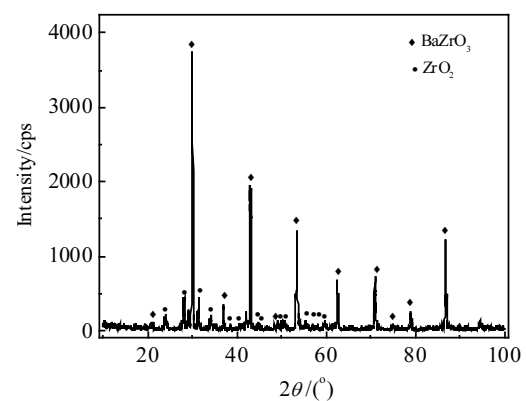


Fig.1 XRD pattern of fused $BaZrO_3$

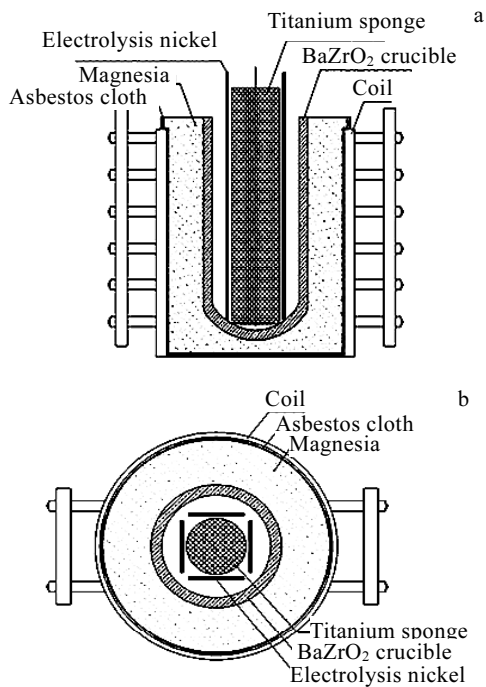


Fig. 2 Schematic illustration of loading structure: (a) front elevation and (b) planform

Ar gas three times after the vacuum degree was evacuated to less than 5×10^{-2} Pa by a diffusion pump. In the melting period, the temperature was increased gradually. The refining temperature was controlled at about 1450°C for 3 min after the alloy was completely melted. Finally, the melt was poured into a graphite mould which was preheated and placed in the furnace, and the TiNi ingot with a mass of 13.5 kg was shaped. After the melting and casting, the samples extracted from the core of alloy ingot were used for chemical analysis, and the alloy ingot was processed into a wire form ($\Phi 1.0$ mm) by homogenizing annealing, forging, rolling and drawing subsequently. Wire samples for property test were collected after different heat treatments as given in Table 1. To compare the fatigue and shape memory properties of samples melted by BaZrO_3 and graphite crucibles, the identical chemical constitution, processing parameters and heat treatments with Qi's work [24] were carried out in this work.

The contents of oxygen and nitrogen were measured by TC-386 Nitrogen-oxygen analyzer, and the carbon contamination was measured by CS-600 Carbon-sulfur determinator. Other chemical compositions were examined by IRIS Advantage ICP-AES type inductive coupled plasma emission spectrometer (ICP). The phase constitution of the as-cast alloy was analyzed by X-ray diffraction (XRD). Samples for optical microscope (OM) and scanning electron microscope (SEM) analyses were prepared using standard metallographic techniques; and the microstructures were revealed by etching with 8% HF-12% HNO_3 -80% H_2O (vol%) solution.

Table 1 Description of different heat treatments for 49.3 Ti-Ni (at%) wires samples used for properties testing

Heat treatment system	Heat treatment description
A	As-processed without heat treatment
B	Water aging at 500°C for 20 min
C	Water aging at 550°C for 20 min
D	Air-cooling at 700°C for 40 min
E	Air-cooling at 850°C for 40 min

1.3 Properties testing

In the following testing experiments, the alloy melted by the graphite crucible was used as a reference and marked as group I [24], and the alloy melted by BaZrO_3 was marked as group II.

The shape memory recovery rates of TiNi SMA were tested using the home-made test apparatus shown in Fig. 3 [24]. In this experiment, samples under heat treatment system D were first loaded to a bending of about 90° and then heated to above 80°C , and every cycle was only preform only once. Besides, each sample has a different deformation amount by selecting moulds in different sizes. The shape memory recovery rates were calculated by Eq. (1) [24], and the deformation amount in the process of bending was calculated by Eq. (2) [24].

$$\eta = (\theta_i - \theta_f) / \theta_i \quad (1)$$

where θ_f is residual angle, $\theta_i - \theta_f$ is recovery angle, θ_i is 90° in every group.

$$\varepsilon = \frac{D/2}{R + D/2} \quad (2)$$

Where D is diameter of TiNi wire, R is curvature radius of column mould.

The home-made test apparatus shown in Fig. 4 is used for testing low cycle bending fatigue (LCBF) behavior [24]. In the experimental process, the bending and recovery of wire samples should be conducted in the same facet. The samples began to bend from block A; the external force began to cancel when the samples touched block B, and the next cycle was conducted after the samples returned to the original position. The deformation amount of TiNi wire was 7% in this experiment, and the water aging was also conducted in the three groups of samples. The first group was under heat treatment system A, the second group was under heat treatment system B, and the last group was under heat treatment system D. Each group was repeated three times to count an average value, and the deviation range was counted.

2 Results and Discussion

2.1 Ingot composition analysis

The main contents of impurities in group II were examined and are listed in Table 2. Table 2 also lists the impurities composition of group I that were melted using the graphite crucible [24].

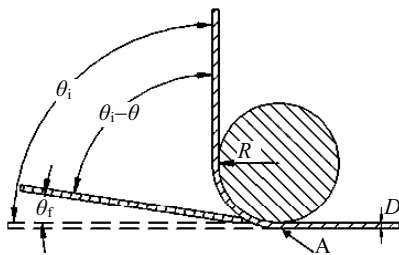
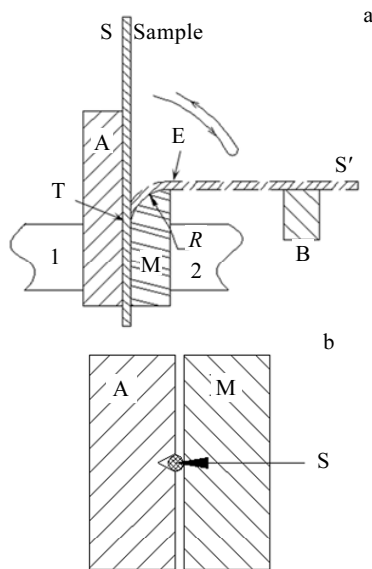


Fig.3 Schematic illustrations of recovery rate test apparatus



F is the fixture used for holding the wire sample; S is wire sample; S' is bended sample; A and B are the started and finished positions of the bending; M is the deformation mould; R is radius of the mould, and 1 and 2 are the contact positions to ensure the bending was repeated fully in the identical paths

Fig.4 Schematic illustrations of endurance bending test apparatus: (a) front elevation and (b) planform

Table 2 shows that the contents of different impurity element in group II can be controlled effectively, the contents of oxygen and nitrogen in the alloy are 560 and 17 $\mu\text{g/g}$, respectively. Under the rush of molten metal at high temperature, the refractory materials will peel off and fall from the surface of crucible. This effect cannot be avoided

in the vacuum induction melting process, resulting in an increase in the element barium, zirconium and oxygen contents. The content of carbon can be negligible in the ingot compared to group I. As introduced in the ASTM F2063-05^[25] for medical devices and surgical implants, the product analysis tolerance for oxygen and nitrogen is 0.004%. Thereby the content of impurity elements is just eligible to biomedical TiNi alloy according to this standard.

Generally speaking, when using the vacuum inducing melting method to produce TiNi alloys, many experimental conditions such as drying of raw materials, high enough vacuum degree, suitable time and temperature in the refining period should be guaranteed, because each of them can affect the experimental results. Meanwhile, to reduce the impurity contents to a lower range and obtain eligible commercial products, other investigations are also being carried out by our group, such as improving the surface quality and thermal stability of BaZrO₃ crucible through adjusting the manufacturing techniques and doping modification.

2.2 Microstructure

Fig.5 presents the Ti-Ni phase diagram and the X-ray diffraction (XRD) pattern of as-cast 49.3Ti-Ni (at%) alloy. As can be seen from Fig.5a, the phase constitution of the as-cast alloy should be a considerable amount of primary NiTi phase and a little Ni₃Ti phase, and the percentage of Ni₃Ti phase is 2.8% in ideal circumstance. As presented in Fig.5b, the phase constitution of the as-cast TiNi alloy is single NiTi phase with B2 (CsCl) type ordered structure. Considering the analysis accuracy of X-Ray diffractometer, the Ni₃Ti and other secondary phases can be barely detectable. XRD results indicate that the as-cast phase constitution is homogeneous and impurity elements do not cause a large deviation in the melting and solidification process.

Foroomehr et al^[26] investigated the property and microstructure of Ti-50at%Ni shape memory alloy produced by vacuum arc remelting (VAR). They found that high segregation of nickel occurred during solidification, resulting in the as-cast microstructure by VAR consisting of variant intermetallic phases of Ti₂Ni, Ni₃Ti, NiTi (B19') and NiTi (B2), as shown in Fig.6. Only after of homogenization annealing at 1000 °C for 4 h, the microstructure can transform to a single TiNi (B2) phase, which is just like the as-cast structure by VIM. Compared to VAR, the microstructure and chemical composition by VIM are more uniform.

Table 2 Impurity composition of TiNi ingot

Sample name	Content of element/wt%						Reference
	Ba	Ca	Zr	C	O	N	
I	-	<0.005	-	0.068	0.048	0.0042	[24]
II	0.00082	<0.005	0.040	0.0061	0.056	0.0017	This work
Standard	None	None	None	≤0.050	≤0.050	≤0.050	ASTM F2063-05 ^[23]

Note: the symbol “-” means the content is lower than the detection limit

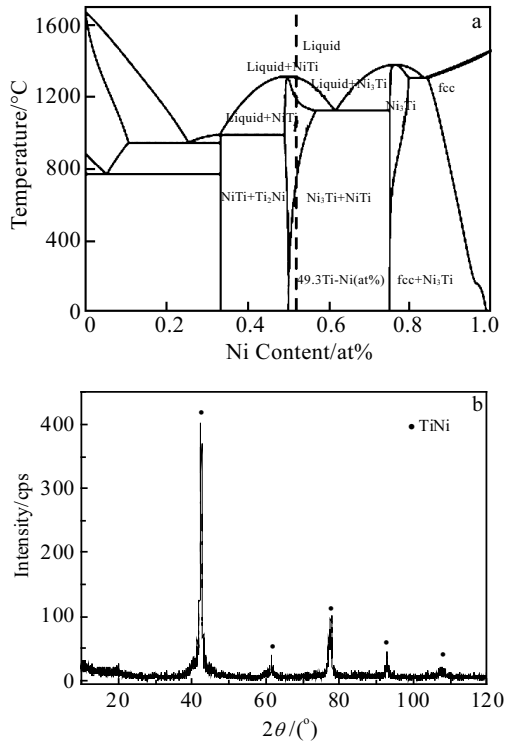


Fig.5 Ti-Ni phase diagram from Pandat software (a) and XRD pattern of as-cast 49.3Ti-Ni (at%) alloy (b)

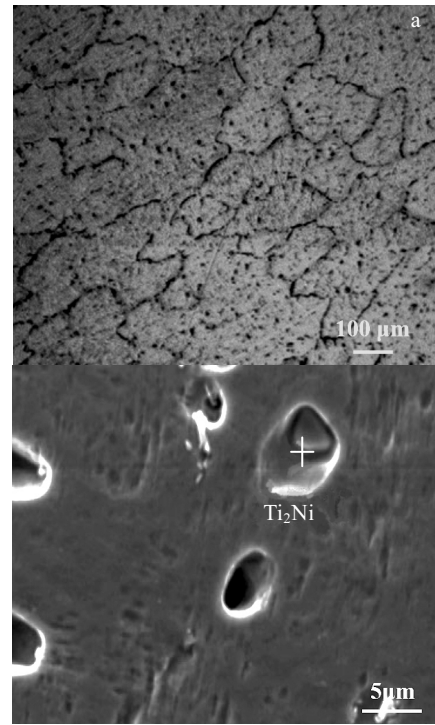


Fig.7 Macrostructure (a) and microstructure (b) of the as cast Ti-50at%Ni alloy produced by VAR method by Foroozmehr et al [26]

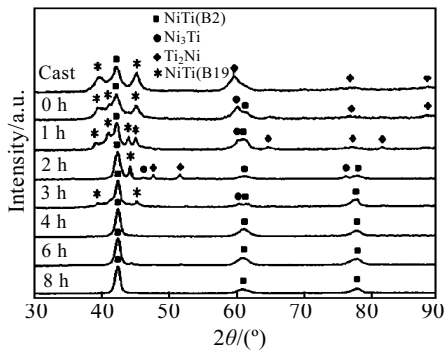


Fig.6 XRD patterns of as-cast, Ti-50at%Ni after homogenized for different time by Foroozmehr et al [26]

Foroozmehr et al [26] studied the macro and microstructure of as-cast Ti-50at%Ni alloy produced by VAR method, which consists mainly of highly segregated and coring products, as shown in Fig.7. Even after 4 h of homogenization, the Ti_2Ni precipitates were still distributed on the grain boundaries.

Fig.8 shows the as-cast structure of 49.3Ti-Ni (at%) SMA melted by VIM in $BaZrO_3$ crucible. As shown in Fig.8, the as-cast structure of the alloy is composed of TiNi matrix phase and lamellar eutectic structures along the straight grain boundaries. Similar eutectic structures of 49.4Ti-Ni (at%) alloy were observed in Sadrnezhad's work [27], when

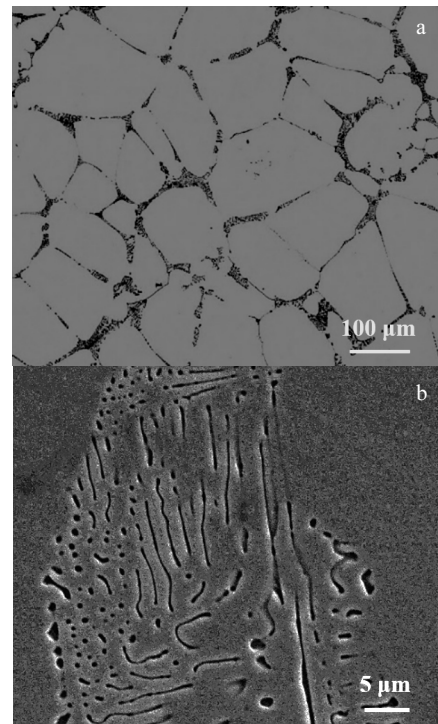


Fig.8 OM (a) and SEM (b) microstructures of as-cast 49.3Ti-Ni (at%) SMA melted by VIM method using $BaZrO_3$ crucible

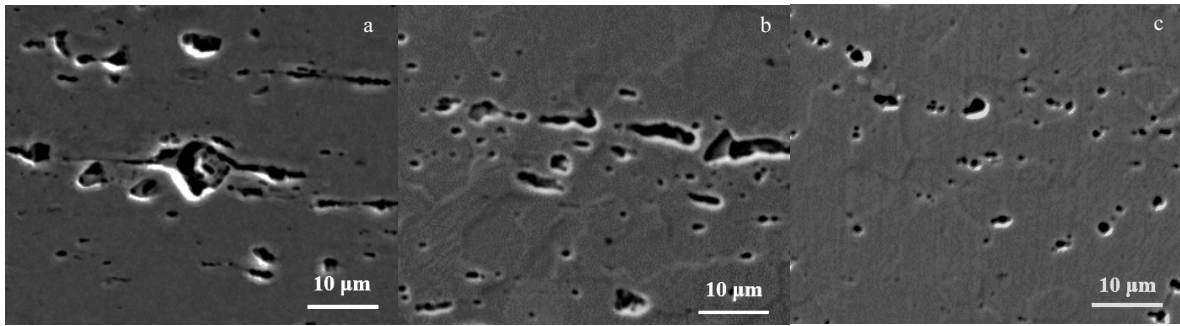


Fig.9 SEM Microstructures of TiNi alloy wires under different heat treatment system: (a) system A, (b) system D, and (c) system E

they investigated the influence of heat treatment on the shape memory effect. Heterogeneous second phase cannot be observed except for eutectic structures. Obviously, vacuum induction melting presents a greater homogeneity in as-cast microstructure. Shape memory (SM) properties are strongly dependent on accurate alloy composition and uniform microstructure. Obtaining alloy ingots with a good chemical and microstructural homogeneity is of great significance for the production of high-quality TiNi SMA^[28].

Fig.9 show SEM microstructures of TiNi alloy wires under different heat treatment systems. As seen in Fig.9a, after homogenization annealing, forging, rolling and drawing processes, the eutectic structure is destroyed during the fabricating process, and there are coarse secondary phases distributed on the TiNi matrix which are deformed and elongated in the deformation direction. As shown in Fig.9b and 9c, the large-size secondary phases are refined in the post deformation annealing at 700 °C for 40 min, and the particle size decreases as the annealing temperature increases. After the alloy wire was hold at 850 °C for 40 min, the particle size is narrowed to below 4 μm. Meanwhile isometric recrystallized grains appear and replaced the fibrous deformed microstructure gradually. These large-size particles will generally transform to smaller sizes during the deformation and heat treatments. Furthermore, these particles are vulnerable during mechanical test and must be refined or modified^[29].

2.3 Shape memory effect

The results of bending test thermo-mechanically treated samples are presented in Fig.10. As seen in Fig.10, the shape memory recovery rate of different samples was decreased with an increasing deformation amount. It is known that shape memory effect of TiNi alloy is the result of an inverse martensite transformation. Since the dislocations impede the transformation from martensite to austenite, an increasing deformation amount will enhance the stability of martensite in the matrix generally, resulting in a rise in the inverse martensitic transformation temperature and the transformation hysteresis^[30].

Meanwhile, samples melted using BaZrO₃ crucible pre-

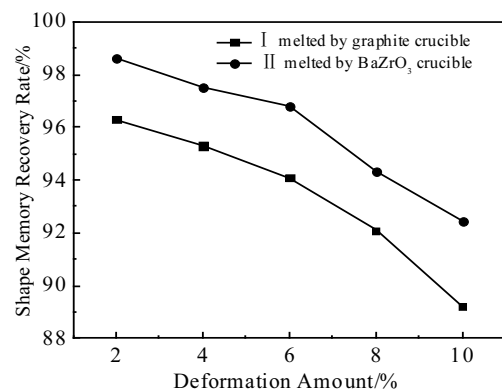


Fig. 10 Variation of shape memory recovery by deformation amount under heat treatment system C

sent higher shape memory recovery rates than that melted by graphite crucible. Since the chemical character of the titanium is quite active at high temperatures, the carbon few to form TiC with the titanium easily in the melting process, which cause a rise in nickel concentration at local regions. In TiNi shape memory alloys, a slight deviation in composition drastically alters the transformation temperatures. For example, 0.1 at% increase in the Ni content can decrease the Ms temperature by more than 10 °C^[23]. Besides, the presence of TiC leads to dislocations tangling, and dislocation density increases in local regions, resulting in an increase in the transformation resistance. Lopez et al^[31] found that a large volume fraction of coarse particle can influence the phase transformation temperature by promoting the martensitic nucleation while act as effective barriers for the propagation of martensite interface. Through comparing the shape memory recovery rates, we can see that a large amount of carbon contaminant can degrade shape memory recovery rate. Although the oxygen content in sample II is 80 μg/g higher, the carbon content in sample I is 600 μg/g than in higher than sample II. The reaction between the graphite crucible and titanium will greatly affect the shape memory properties of TiNi alloys.

2.4 Fatigue life

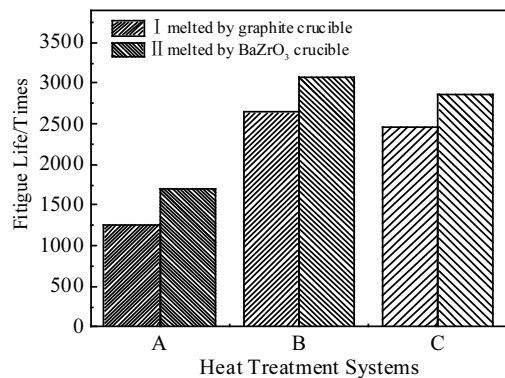


Fig. 11 Fatigue life of the samples under different heat treatment systems

The effect of annealing temperature on fatigue life is shown in Fig.11. The samples melted by BaZrO₃ crucible were fabricated and heat treated in the identical manner with ones melted by graphite crucible. As seen in Fig.11, samples melted by BaZrO₃ crucible present higher fatigue life than by graphite crucible under different heat treatments. Nayan et al^[23] showed the as-cast microstructure of TiNi alloys melted by VIM in graphite crucible. A large amount of large TiC precipitates distributed in the grain interior and grain boundaries can be clearly observed. As shown in Table 2, the total content of carbon, oxygen and nitrogen in the alloy prepared by graphite crucible was much higher than that in the alloy prepared by BaZrO₃ crucible. Part of the carbon dissolved in the TiNi matrix which mainly affected the phase transformation temperature, and the other part exceeding the upper limit of solubility will easily form a TiC phase with titanium. The formation of TiC led to a deviation from the equi-atomic NiTi composition and as a consequence, Ti₂Ni and Ni₄Ti₃ phase precipitated accordingly^[23, 28]. The oxygen solubility of the TiNi phase is about 0.045 at%, and the Ti₂NiO_x phase is the only phase in the alloy that can contain oxygen. The Ti₂NiO_x phase can also lead to the formation of non-stoichiometric compounds on NiTi grain boundaries, such as TiNi₃ and the Ti₂Ni, which significantly decrease workability^[32]. The presence of these large precipitates will lead to the accumulation of defects, and these areas of high defects density will transform to fatigue sources in the cyclic loading process, resulting in a decline in fatigue life^[33,34].

It's widely accepted that the major drawback of vacuum induction melting TiNi alloy using the graphite crucible is the carbon contamination from the crucible. Compared to BaZrO₃ crucible, the oxygen content was not significantly reduced using graphite crucible, and the carbon content also reached 680 μg/g. In contrast, the BaZrO₃ crucible can ef-

fectively prevent the reaction between the refractory and the titanium melt during the melting process, and the total content of impurity element in the alloy can be controlled within a lower range, thereby avoiding shape memory properties and fatigue properties degrading.

3 Conclusions

1) The 49.3Ti-Ni (at%) SMA is fabricated successfully by vacuum induction melting in 25 kg-grade home-made BaZrO₃ crucible. The contents of oxygen and nitrogen in the alloy are 560 and 17 μg/g, respectively, and only little of Ba and Zr exists. Besides, other impurities elements (C, Ca) are almost negligible. The contents of impurity elements are just eligible to medical devices and surgical implants according to the standard ASTM F2063-05.

2) The microstructure of 49.3Ti-Ni (at%) SMA melted by VIM in BaZrO₃ crucible consists of NiTi matrix phase and little Ni₃Ti phase. Compared to the highly segregated and cored as-cast structure by VAR, the chemical composition of ingot by VIM is more uniform and accurate.

3) The 49.3Ti-Ni (at%) SMA melted by VIM using BaZrO₃ crucible presents higher shape memory effect and fatigue life than using graphite crucible. The best shape memory recovery rate can reach 98.62% under 2% deformation after aging at 550 °C for 20 min and water quenching, the best average fatigue life can reach 3072 times after aging at 500 °C for 20 min and water quenching.

References

- Jaronie M J, Martin L, Aleksandar S et al. *Materials and Design*[J], 2014, 56: 1078
- Otsuka K, Wayman C M. *Shape Memory Materials*[M]. New York: Cambridge University Press, 1999: 1
- Otsuka K, Ren X. *Intermetallics*[J], 1999, 7(5): 511
- Van Humbeeck J. *Materials Science and Engineering A*[J], 1999, 273: 134
- Duerig T W, Pelton A, Stöckel D. *Materials Science and Engineering A*[J], 1999, 273: 149
- Song Peng, Zhu Ying, Guo Wei et al. *Rare Metal Materials and Engineering*[J], 2013, 42(S2): 6
- Welsch G, Boyer R, Collings E W. *Materials Properties Handbook: Titanium Alloys*[M]. Ohio: ASM International, 1993: 1035
- Yin Y, Kakeshita T, Choi M S et al. *Journal of Alloys and Compounds*[J], 2008, 464(1-2): 422
- Takeshita H T, Tanaka H, Kuriyama N et al. *Journal of Alloys and Compounds*[J], 2000, 311(2): 188
- Sadrnezhad S K, Raz S B. *Metallurgical and Materials Transactions B*[J], 2005, 36(3): 395
- Faran E, Gotman I, Gutmanas E Y. *Materials Science and Engineering A*[J], 2000, 288(1): 66
- Li Qian, Yang Hailin, Wan Jianming et al. *Rare Metal Mate-*

- rials and Engineering[J], 2013, 42(5): 1023 (in Chinese)
- 13 Zhao Dan, Yang Yi, Yang Gang et al. *Rare Metal Materials and Engineering*[J], 2016, 45(7): 1816
- 14 Kartavykh A V, Tcherdyntsev V V, Zollinger J. *Materials Chemistry and Physics*[J], 2009, 116(1): 300
- 15 Gomes F, Puga H, Barbosa J et al. *Journal of materials science*[J], 2011, 46(14): 4922
- 16 Lin K, Lin C. *Scripta Materialia*[J], 1998, 39(10): 1333
- 17 Zhang Z, Xing F Y, Zhu M et al. *Materials Science Forum*[J], 2013, 765: 316
- 18 Degawa T. *Bull. Jpn Inst Met*[J], 1988, 27(6): 466
- 19 Erb A, Walker E, Flükiger R. *Physica C: Superconductivity*[J], 1996, 258(1): 9
- 20 Gopalan S, Virkar A V. *Journal of the American Ceramic Society*[J], 1999, 82(10): 2887
- 21 Xing Fangyuan, Chen Guangyao, Zhu Kailiang. *Journal of Taiyuan University of Technology*[J], 2014,45(2): 172 (in Chinese)
- 22 Schafföner S, Aneziris C G, Berek H et al. *Journal of the European Ceramic Society*[J], 2013, 33(15-16): 3411
- 23 Nayan N, Govind, Saikrishna C N et al. *Materials Science and Engineering A*[J], 2007, 465: 44
- 24 Qi Baode, Miao Weidong, Wang Jiangbo. *Chinese Journal of Rare Metals*[J], 2008(2): 252 (in Chinese)
- 25 *Standard Specification for Wrought Nickel-Titanium Shape Memory Alloys for Medical Devices and Surgical Implants*, ASTM F2063-05[S], ASTM International, West Conshohocken, PA, 2005
- 26 Foroozmehr A, Kermanpur A, Ashrafizadeh F et al. *Materials Science and Engineering A*[J], 2011, 528(27): 7952
- 27 Sadrnezhad K, Mashhadi F, Sharghl R. *Materials and Manufacturing Processes*[J], 1997, 12(1): 107
- 28 Frenzel J, Zhang Z, Neuking K et al. *Journal of Alloys and Compounds*[J], 2004, 385(1-2): 214
- 29 Yen F, Hwang K. *Materials Science and Engineering A*[J], 2011, 528(15): 5296
- 30 Zhao Liancheng, Cai Wei, Zheng Yufeng. *Shape Memory Effect and Superelasticity in Alloys*[M]. Beijing: National Defence Industry Press, 2002: 161 (in Chinese)
- 31 Lopez H F, Salinas A N H C. *Metallurgical and Materials Transactions A*[J], 2001, 32A: 717
- 32 Mehrabi K, Bahmanpour H, Shokuhfar A et al. *Materials Science and Engineering A*[J], 2008, 481-482: 693
- 33 Li Yanfeng, Mi Xujun, Gao Baodong et al. *Materials Review*[J], 2007(6): 84 (in Chinese)
- 34 Guangbin R, Jianqiu W, Enhou H et al. *Acta Metallurgica Sinica*[J], 2002, 38(6): 575 (in Chinese)

利用 BaZrO₃ 坩埚制备钛镍形状记忆合金组织及性能的研究

高鹏越¹, 黎政¹, 朱明³, 陈光耀¹, Wajid Ali¹, 李明阳¹, 秦子威^{1,2}, 汪洪斌^{1,2}, 鲁雄刚^{1,2}, 李重河^{1,2}

(1. 上海大学 高品质特殊钢冶金与制备国家重点实验室 上海市钢铁冶金新技术开发应用重点实验室, 上海 200072)

(2. 上海特种铸造工程技术研究中心, 上海 200072)

(3. 北京有色金属研究总院, 北京 100088)

摘要: TiNi 形状记忆合金由于其优良的合金性能, 而成为商业化应用最为广泛的形状记忆合金。利用 25 kg 级自制 BaZrO₃ 坩埚制备了 49.3Ti-Ni (at%) 合金, 并将铸态合金加工成为直径为 1 mm 的丝材。利用 XRD、氮氧化物分析仪等分析测试手段对合金的化学成分及物相组成进行研究分析, 利用扫描电镜、光学显微镜对合金的显微组织进行观察, 利用两台自制设备对合金丝材的形状记忆回复率及疲劳性能进行分析测试。实验结果表明, 利用 BaZrO₃ 坩埚对制备的钛镍合金的氧、氮含量能够分别达到 560 和 17 μg/g, 杂质元素含量满足 ASTM 对于医用植入物以及医疗器械的标准要求; 相对真空电弧熔炼, 利用 BaZrO₃ 坩埚感应熔炼制备的 TiNi 合金化学成分更加准确均匀; 与石墨坩埚感应熔炼相比, 利用 BaZrO₃ 坩埚制备的 TiNi 合金丝材表现出更为优良的形状记忆回复率和抗疲劳性能, 其形状记忆回复率在 550 °C 保温 20 min 淬火后, 变形量为 2% 时能够达到 98.62%, 其疲劳性能在 500 °C 保温 20 min 淬火后能够达到 3072 次。

关键词: BaZrO₃ 坩埚; TiNi 形状记忆合金; 微观组织; 合金性能

作者简介: 高鹏越, 1990 年生, 博士生, 上海大学材料科学与工程学院, 上海 200072, 电话: 021-56332934, E-mail: gaopenyue@i.shu.edu.cn